

## Article

# Prediction of Changes in Blood Parameters Induced by Low-Frequency Ultrasound

Vytautas Ostasevicius <sup>1,\*</sup>, Agnė Paulauskaite-Taraseviciene <sup>2</sup>, Vaiva Lesauskaite <sup>3</sup>, Vytautas Jurenas <sup>1</sup>, Vacis Tatarunas <sup>3</sup>, Edgaras Stankevicius <sup>4</sup>, Agilė Tunaityte <sup>5</sup>, Mantas Venslauskas <sup>1</sup> and Laura Kizauskiene <sup>6</sup>

<sup>1</sup> Institute of Mechatronics, Kaunas University of Technology, Studentu Street 56, LT-51424 Kaunas, Lithuania; vytautas.jurenas@ktu.lt (V.J.); mantas.venslauskas@ktu.lt (M.V.)

<sup>2</sup> Department of Applied Informatics, Kaunas University of Technology, Studentu Street 50, LT-51368 Kaunas, Lithuania; agne.paulauskaite-taraseviciene@ktu.lt

<sup>3</sup> Laboratory of Molecular Cardiology, Institute of Cardiology, Lithuanian University of Health Sciences, A. Mickevicius Street 9, LT-44307 Kaunas, Lithuania; vaiva.lesauskaite@lsmu.lt (V.L.); vacis.tatarunas@lsmu.lt (V.T.)

<sup>4</sup> Institute of Physiology and Pharmacology, Lithuanian University of Health Sciences, A. Mickevicius Street 9, LT-44307 Kaunas, Lithuania; edgaras.stankevicius@lsmu.lt

<sup>5</sup> Preclinical Research Laboratory for Medicinal Products, Institute of Cardiology, Lithuanian University of Health Sciences, Sukileliu Street 13, LT-50166 Kaunas, Lithuania; agile.tunaityte@lsmu.lt

<sup>6</sup> Department of Computer Sciences, Kaunas University of Technology, Studentu Street 50, LT-51368 Kaunas, Lithuania

\* Correspondence: vytautas.ostasevicius@ktu.lt

**Abstract:** In this study, we reveal the influence of low-frequency ultrasound on erythrocyte and platelet aggregation. Furthermore, we show that the consequences of sonication of blood samples can be predicted using machine learning techniques based on a set of explicit parameters. A total of 300 blood samples were exposed to low-frequency ultrasound of varying intensities for different durations. The blood samples were sonicated with low-frequency ultrasound in a water bath, which operated at a frequency of  $46 \pm 2$  kHz. Statistical analyses, an ANOVA, and the non-parametric Kruskal–Wallis method were used to evaluate the effect of ultrasound on various blood parameters. The obtained results suggest that there are statistically significant variations in blood parameters attributed to ultrasound exposure, particularly when exposed to a high-intensity signal lasting 180 or 90 s. Furthermore, among the five machine learning algorithms employed to predict ultrasound's impact on platelet counts, support vector regression (SVR) exhibited the highest prediction accuracy, yielding an average MAPE of 10.34%. Notably, it was found that the effect of ultrasound on the hemoglobin (with a  $p$ -value of  $< 0.001$  for MCH and MCHC and 0.584 for HGB parameters) in red blood cells was higher than its impact on platelet aggregation (with a  $p$ -value of 0.885), highlighting the significance of hemoglobin in facilitating the transfer of oxygen from the lungs to bodily tissues.

**Keywords:** blood samples; acoustic intensity; platelet aggregation; hematological disorders; Kruskal–Wallis test; support vector regression



**Citation:** Ostasevicius, V.; Paulauskaite-Taraseviciene, A.; Lesauskaite, V.; Jurenas, V.; Tatarunas, V.; Stankevicius, E.; Tunaityte, A.; Venslauskas, M.; Kizauskiene, L. Prediction of Changes in Blood Parameters Induced by Low-Frequency Ultrasound. *Appl. Syst. Innov.* **2023**, *6*, 99. <https://doi.org/10.3390/asi6060099>

Academic Editor: Dorota S. Temple

Received: 28 September 2023

Revised: 19 October 2023

Accepted: 25 October 2023

Published: 26 October 2023



**Copyright:** © 2023 by the authors. Licensee MDPI, Basel, Switzerland. This article is an open access article distributed under the terms and conditions of the Creative Commons Attribution (CC BY) license (<https://creativecommons.org/licenses/by/4.0/>).

## 1. Introduction

### 1.1. Related Work

The effect of ultrasound on platelet aggregation has been highlighted in studies [1–6]. Platelets perform many functions in the human body. They participate in the formation of blood clots, interacting with fibrin and stopping blood loss from damaged blood vessels. As stated in [1], low-intensity ultrasound in combination with a dose of synthetic particles accelerates clot density and stiffness improvements, suggesting that this treatment may lead to better healing of fractures and injuries. Another study [2] shows that early ( $\leq 5$  months) healing of patients with venous stasis and diabetic foot ulcers was favorably influenced by low-frequency ultrasound. Most published studies of platelet aggregation have been

performed using chemical stimulation procedures, but ultrasound stimulation may be more effective [3]. The results in [4] show that platelet aggregation after exposure to low-frequency (22 kHz) and low-intensity (from 1.0 to 8.8 W/cm<sup>2</sup>) ultrasound depends on the intensity and time of exposure; in addition, platelet aggregation occurs only when the platelet medium contains calcium ions (Ca<sup>2+</sup>). A more accurate method was proposed to investigate platelet function, atherosclerotic plaques, and ischemic heart disease in [5]. The results in article [6] show that non-invasive contrast-enhanced ultrasound molecular imaging with targeted microbubbles can detect not only activated platelets in the vascular endothelium, but also the severity of atherosclerosis damage.

The effects of ultrasound in biology and blood cells have been examined in research conducted by the authors of [7–10]. The extent of damage to atherosclerotic tissue and the presence of platelets on the surface of the endothelium were assessed both from histological and immunohistochemical points of view. As a result of research on animals (rats), ultrasound was found to reduce inflammation by reducing the amount of fibrinogen in the blood [7]. The effect of ultrasound on fibrinogen and coagulation and fibrinogenolysis processes in an in vitro system was investigated by the authors of [8]. A study [9] analyzed the mechanical effect (immediate lysis) and biological effects (cell survival, apoptosis, cell cycle) in cells exposed to different ultrasound frequencies. It was found that cell survival decreased with increasing ultrasound intensity. From these findings, a conclusion can be drawn regarding the advantages of low-frequency ultrasound. As reported in paper [10], low-intensity pulsed ultrasound can accelerate the healing of fresh fractures, improve soft tissue regeneration, and suppress inflammatory reactions.

The advantages of artificial intelligence are described in [11–20]. Every year, machine learning algorithms gain increasing prominence in the (bio)medical sector, effectively addressing the most crucial tasks, such as disease identification [11], classification, and prediction and a variety of investigations involving blood samples [12]. A study [13] showed that powerful machine learning techniques can classify, detect, and predict blood cell subtypes and changes in blood cell count, shape, texture, and color. Study [14] briefly reviews and discusses the philosophy, possibilities, and limitations of artificial neural networks in medical diagnostics. Blood analysis, as one of the main detectors of diseases, provides many different parameters that show unequivocal evidence of the existence of a disease [15]. The use of machine learning to predict platelet activation and cell surface dynamics [16] focuses on the question of whether simple geometric features obtained from platelets scanned via standard light microscopy techniques are useful predictors of platelet shape replacement. The authors of [17] presented an in vitro microarray analysis based on aggregated platelet detection using time-lapse optofluidic microscopy and machine learning, which allowed for the identification and counting of aggregated platelets based on their morphology in a short time. Another work [18] used machine learning, ultrasound, and blood test data to predict relapses in patients with rheumatoid arthritis. The application of artificial intelligence methods is clearly relevant in the field of hematopathology. In [19], the authors present an intelligent deep learning algorithm that was used to process microscopic images of blood smears in order to predict the presence of leukemia cells using a convolutional neural network (CNN). The research was carried out on open-source data and showed the promising potential of the proposed approach. In a broader context, recent advances in artificial intelligence in hematopathological microscopy are discussed in [20]. This work highlights the potential of AI technologies to improve hematopoietic cell identification, data resolution, and information quality. It also discusses the limitations and indicates possible directions for future research.

### 1.2. Research Objectives

Although most ongoing research papers are related to blood platelet aggregation, it is obvious that there is a need to investigate the influence of ultrasound on other blood parameters. The primary purpose of this paper is to delve deeper into this specific area, extending the previous initiated research and aiming to explore the effects of low-frequency

ultrasound (40–50 kHz) with varying intensities (10–150 mW/cm<sup>2</sup>) on diverse blood parameters measured using a modern blood analyzer. Given the plethora of measured blood parameters provided by the blood analyzer, computerized methods were employed for comprehensive analysis of the resulting data array. This enabled a more thorough evaluation of the changes in certain blood parameters resulting from the patient's health condition when influenced by ultrasound. The effect of ultrasound on blood parameters was assessed individually by comparing each patient's non-ultrasound control sample with samples exposed to different ultrasound regimes. To make sure that the changes in certain blood parameters detected by the analyzer were adequate and reliable, a comparative laboratory blood coagulation study was performed. This involved the stimulation of blood with epinephrine with additional exposure to ultrasound. The results demonstrated that ultrasound stimulation led to an acceleration of the blood clotting process.

## 2. Materials and Methods

### 2.1. Sonication of Blood Samples

Blood sonication was performed using water bath sonication technology with a CT-400 ultrasonic cleaner (Wah Luen Electronic Co., Ltd., Shantou, China), which was operated at a frequency of  $46 \pm 2$  kHz with different intensities and durations of ultrasound. To ensure the ultrasound frequency, the ultrasonic intensity was measured and parameters were kept constant during each stage of the experiment; tests were carried out using a hydrophone HCT-0320 connected to an acoustic cavitation meter MCT-2000 (Ondo Corp., Novi, MI, USA). Since ultrasound with electric power leads to higher temperatures that might degrade the blood samples, the temperature was strictly monitored and controlled at  $25 \pm 2$  °C. The sonication platform is shown in Figure 1. The water temperature in the ultrasonic bath was controlled at  $25 \pm 2$  °C. Water temperature fluctuations were caused by the periodic operation of the ultrasonic bath. The study measured the highest rise in water temperature within the bath over a continuous period of 180 s while generating ultrasound at an intensity of 100–150 mW/cm<sup>2</sup>. Following each ultrasound bath operation, a pause in experiments was implemented until the water temperature within the bath returned to 23 °C.

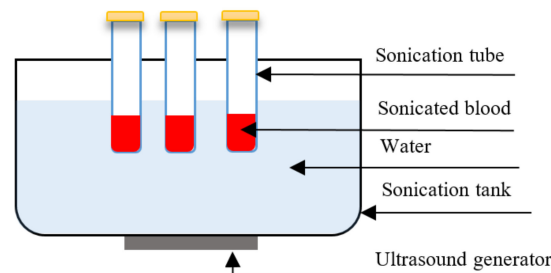


**Figure 1.** Schematic diagram of the blood sample sonication setup.

### 2.2. Investigation of Hematological Parameters

Certified nurses collected blood from lung disease patients, and the blood was placed into 3 mL Vacuette K2E K2EDTA  $13 \times 75$  tubes with lavender caps and black rings and equally divided into 7 parts, so that each part (~0.43 mL) was exposed to ultrasound (US). The Swelab Alfa system (Boule Medical AB, Stockholm, Sweden) [21] used in this research is an automated hematology analyzer for in vitro diagnostics under laboratory conditions. The Swelab Alfa analyzer was used to determine red blood cell (RBC) counts; the mean cell volume of red cells (MCV); the red cell distribution relative and absolute volumes (RDW%, RDWa); hematocrits (HTCs); the platelet count (PLT); the mean platelet volume (MPV); the platelet distribution width (PDW); plateletcrits (PCTs); the platelet large cell ratio (LPCR); white blood cells (WBCs); hemoglobin (HGB); mean corpuscular hemoglobin (MCH); the mean corpuscular hemoglobin concentration (MCHC); lymphocytes (LYMs); granulocytes (GRANs); the minimum inhibitory dilution (MID); the lymphocyte percentage (LYM%); the granulocyte percentage (GRA%); and the mid-sized white cell percentage (MID%).

All experiments with patient blood were carried out within the first hour after blood collection. The characteristics of the low-frequency ultrasound used on the blood samples are presented in Table 1.

**Table 1.** Characteristics of low-frequency ultrasound used on blood samples.

Sonication Mode	Ultrasound Exposure, s	Ultrasound Intensity, mW/cm <sup>2</sup>	Electric Power, W	Ultrasound Frequency, kHz
K	0	0	0	0
A	90	100–150	60	48
B	180	100–150	60	48
C	90	50–70	35	44
D	180	50–70	35	44
E	90	5–12	10	44
F	180	5–12	10	44

### 2.3. Investigation of Platelet Aggregation

To demonstrate that the selected frequency and intensity of ultrasound induce platelet activation in a dose-dependent manner, a single individual's blood was analyzed utilizing a platelet aggregometer. Two blood samples were collected for testing purposes. One sample served as the control, without any ultrasound exposure, and instead was treated with epinephrine (adrenaline) to induce platelet aggregation. Another sample was divided into 4 tubes and exposed to ultrasound for varying durations and intensities. It was exposed to ultrasound for 90 s. or 180 s., and after exposure, it was treated with epinephrine to induce platelet aggregation. The ultrasound tests were carried out at different ultrasound signals, i.e., some samples were tested at an electric power of 35 W (US intensity ~50–70 mW/cm<sup>2</sup>), as shown in Table 1, and others were tested at 60 W (US intensity ~100–150 mW/cm<sup>2</sup>). The time and frequencies of 44 kHz were the same to ensure that the ultrasound effect would not be harmful. The platelet aggregation test was conducted at the Laboratory of Molecular Cardiology, Institute of Cardiology, Lithuanian University of Health Sciences, located in Kaunas, Lithuania. The test followed the established classical Born method and utilized a semi-automatic CE IVD certified TA-8V platelet aggregometer from SD Medical (Frouard, France). Platelet aggregation was assessed by comparing the intensity of light transmission between platelet-rich and platelet-poor plasma samples after induction with epinephrine (adrenaline). The transmission of platelet-poor plasma was considered as 100%. The final concentration of epinephrine was 10 µM (Chrono-Log, Havertown, PA, USA). Preparation of platelet-rich plasma was carried out by centrifuging whole blood at 100× *g* for 15 min. Platelet-poor plasma was prepared by centrifuging platelet-rich plasma at 1000× *g* for 30 min. An AFI LISA 2.5 L refrigerated centrifuge (Château-Goutier, France) was used to prepare blood samples. The aggregation of platelets was measured as % Agr.

### 2.4. Kruskal-Wallis Test

The Kruskal-Wallis test is a popular non-parametric statistical test used in medicine to compare the distribution of a continuous variable among multiple groups or treatments [22–24]. It is often used when the assumptions of parametric tests, such as ANOVA, cannot be met or in such cases when the data are not normally distributed or the variances are not equal. The Kruskal-Wallis test compares the sums of the ranks among the groups. If the sums of the ranks differ significantly among the groups, then it can be concluded that at least one group is different from the others [25]. When the null hypothesis of the test is rejected at the user-defined significance level  $\alpha$ , it indicates that at least one of the groups being compared exhibits a statistically significant difference from the others concerning the dependent variable under investigation. Multiple comparison procedures can be used to identify where the differences lie among the populations. Pairwise multiple comparisons compare each pair of groups to determine which groups are significantly different, while the stepwise stepdown procedure is a sequential testing procedure that adjusts the multiple comparisons to reduce the probability

of a type I error. The Kruskal-Wallis method is usually applied to three or more independent groups, but can also be applied to two groups, with a sample size of at least 5 instances in each group. The ranks of the data are used to calculate the test statistic  $H$  as follows:

$$H = \frac{12}{N(N+1)} \sum_{i=1}^k \frac{R_i^2}{n_i} - 3(N+1), \quad (1)$$

where  $N$  is the total number of sample size,  $k$  is the number of groups,  $R_i$  is the sum of ranks for group  $i$ , and  $n_i$  is the sample size of group  $i$ .

This study uses Dunn's test, which performs a pairwise comparison between each independent group and indicates which groups are statistically significantly different at a given confidence level  $\alpha$ . A significance level of 0.05 ( $\alpha = 0.05$ ) is the threshold for rejecting the null hypothesis and confirming the alternative hypothesis. The test uses the average ranks of each group's scores from the Kruskal-Wallis test as an approximate exact statistic for the rank sum test. The test statistic is calculated based on the differences between the mean ranks of the groups and a conclusion is drawn from these differences. When multiple comparisons are made at the same time, it is important to control the (Type I) error rate. One way to do this is to adjust the  $p$ -values obtained from multiple comparisons. A common approach to this is Bonferroni adjustment, also used in our study.

### 2.5. Platelet Number Prediction by Machine Learning

Different measures of accuracy were calculated from the experiments, i.e., the mean squared error ( $MSE$ ), the root mean square error ( $RMSE$ ), and the mean absolute percentage error ( $MAPE$ ) [26]. The  $MSE$  is a measure representing the average of the squared difference between actual and predicted values in a dataset. The  $RMSE$  is just the square root of the root mean square error, the only difference being that the  $MSE$  measures the variance of the residuals, while the  $RMSE$  measures the standard deviation of the residuals.

$$RMSE = \sqrt{MSE}, \text{ where } MSE = \frac{1}{n} \sum_{t=1}^n |y_t - \hat{y}_t|^2 \quad (2)$$

where  $n$ —number of time points,  $y_t$ —the actual value at a given time  $t$ ,  $\hat{y}_t$ —the predicted value, and  $t$ —observation in a dataset.

The  $MAPE$  also evaluates the accuracy of a model's predictions, but it measures the average absolute percentage difference between the predicted and actual values:

$$MAPE = \frac{100\%}{n} \sum_{t=1}^n \left| \frac{y_t - \hat{y}_t}{y_t} \right| \quad (3)$$

## 3. Results

### 3.1. Platelet Aggregation

The results of a blood test with a platelet aggregometer (Figure 2) conducted with epinephrine can also show the suppression of other receptors. The results showed that in the absence of ultrasound, the maximum platelet aggregation recorded was 104% (Figure 2a). Conversely, when sonicated with ultrasound, 100% platelet aggregation was not observed (Figure 2b). Instead, a gradual decrease in platelet aggregation was observed as follows: 95% at an ultrasound intensity of 100–150  $mW/cm^2$ , 92% at an ultrasound intensity of 100–150  $mW/cm^2$  with a duration of 90 s, 86% at an ultrasound intensity of 50–70  $mW/cm^2$ , and 80% at an ultrasound intensity of 50–70  $mW/cm^2$ .

The test results shown in Figure 2 indicate that the process of blood platelet aggregation initiates faster in sonicated samples compared to the sample treated only with epinephrine (adrenaline). For the sonicated samples, 10% platelet aggregation was achieved within 1 min and 40% aggregation was achieved within 2 min after induction of platelet aggregation with epinephrine. For the blood samples treated only with epinephrine (adrenaline), 5% platelet aggregation was achieved within 1 min and 10% aggregation was achieved within

2 min. In vitro [3], it was found that ultrasound produces more stable platelet aggregates than a natural platelet aggregation stimulant. Ultrasound-induced platelet aggregation holds promise as a potential solution to platelet receptor (P2Y<sub>12</sub> receptor) issues, such as defective responses to soluble agonists [27], and as an effective bleeding control.

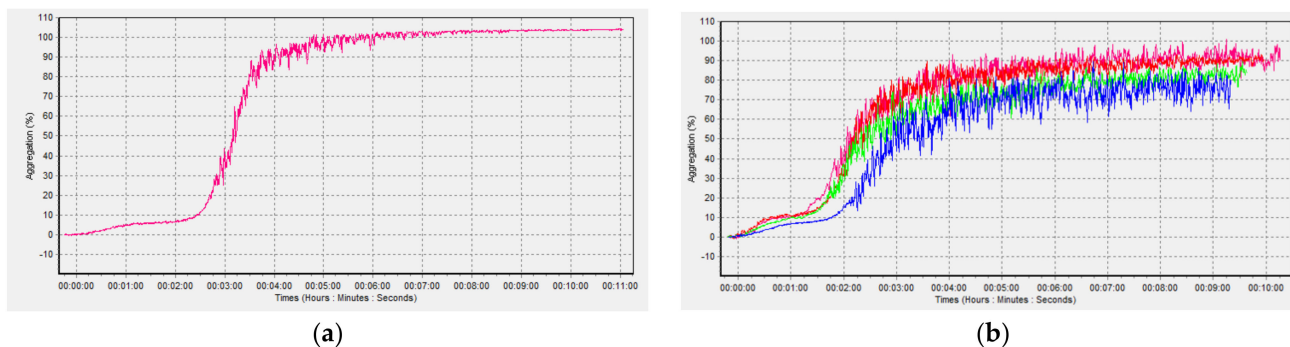


**Figure 2.** Blood platelet aggregation with epinephrine (a) and low-frequency ultrasound (b) in vitro. In (b), two samples are sonicated with ultrasound at 60 W electric power (pink, red) and two samples are sonicated with ultrasound at 35 W electric power (green, blue).

### 3.2. Blood Analysis

Blood samples from 10 (of 42) patients were exposed to six different low-frequency ultrasound modes (Table 1) and changes in 20 blood parameters were identified. The blood of each patient was sonicated under six different ultrasound intensities and time variables (A, B, C, D, E, F), in addition to not being exposed to ultrasound (K). To ensure the statistical validity of our analyses, we assessed the normality of the data using the Kolmogorov-Smirnov test. In cases where significant deviations from normality were detected, suitable transformations were applied to address this issue. Subsequently, paired sample *t*-tests were conducted to compare means between groups, and if significant differences were observed, an ANOVA was performed to evaluate the overall significance. These steps were taken to meet the assumptions of the statistical tests and ensure the reliability of our data analysis.

A repeated-measure ANOVA was performed to compare the effect of different ultrasound exposure conditions (Table 1) on different blood parameters. The ANOVA results revealed that there was a statistically significant (*p*-value < 0.05) difference in 15 blood parameters between at least two groups. MATLAB R2018a was used to conduct statistical analyses for these 15 parameters (Table 2). The *F*-statistic is the ratio of the mean squared errors, where *d*<sub>1</sub> = 40 (for the numerator) and *d*<sub>2</sub> = 6 (for the denominator).

**Table 2.** Repeated-measure ANOVA results.

Parameter:	<i>F</i> <sub>40,6</sub>	<i>p</i> -Value
RBC	13.80	<0.01
MCV	12.51	<0.01
HCT	12.61	<0.01
MPV	14.58	<0.01
PDW	15.20	<0.01
LPCR	15.31	<0.01
WBC	29.43	<0.01
HGB	2.25	0.039
MCH	17.34	<0.01
MCHC	2.53	0.021
LYM	16.98	<0.01
GRAN	32.88	<0.01
LYM%	13.52	<0.01
GRA%	7.29	<0.01
MID%	23.49	<0.01

A multiple comparisons test showed that the mean value of 49 ultrasound conditions was significantly different from the control group. Primarily higher-power ultrasound had the greatest effect on test parameters.

### 3.3. Statistical Analysis

We used a Kruskal-Wallis test with Dunn’s post hoc test to determine whether there was a significant difference in the effect of ultrasound (in terms of different intensities and durations) on different blood parameters. In the table below, each row represents the null hypothesis that the distribution of the two samples is the same. When there is no evidence to reject the null hypothesis, then there is no significant difference, meaning that ultrasound has no effect (or a very small effect) on a particular blood parameter. Otherwise, if the null hypothesis is rejected, this indicates that there is a significant difference between the values of the blood parameters affected by the ultrasound signals. Table 3 shows that for 11 out of 20 parameters, the impact of the ultrasound signals (six different ultrasound conditions) is statistically significant ( $p$ -value is  $<0.05$ ).

**Table 3.** Kruskal–Wallis null hypothesis test results.

Blood Parameters with $p$ -Value $< 0.05$										
RBC	HTC	MPV	PDW	LPCR	WBC	MCH	MCHC	GRA(%)	GRAN	MID(%)
$<0.001$	$<0.001$	0.037	0.044	0.015	0.010	$<0.001$	$<0.001$	0.006	0.002	$<0.001$
Blood Parameters with $p$ -Value $> 0.05$										
RDW	MCV	PLT	PCT	HGB	LYM	MID	RDWa	LYM(%)		
0.990	0.842	0.885	0.808	0.584	0.166	0.467	0.977	0.157		

The diagrams presented in Figure 3 show the results of the Kruskal–Wallis test for different blood parameters with a  $p$ -value of  $>0.05$  (null hypothesis is retained), starting from the baseline value and affected by ultrasound. The notations of the ultrasound set for the sonication of the blood samples are presented on the horizontal axis, varying in strength (C—control/no US, high—H, medium—M, low—W) and duration (90 s and 180 s).

The changes in RDW values after exposure of the blood to ultrasound are very minor, with a slightly larger increase observed when exposed to the highest ultrasound signal for 180 s (180 H). By exposing the blood to a high ultrasound signal for 180 s, we can see that the set of recorded RDW values are outside the normal range. However, the median line between all sets, except 180 H, is almost straight. As we can see, the MCV values are almost non-sensitive to the ultrasound signal, and all values in this blood set are within the normal range (75–100).

A similar situation can be observed with parameters such as HGB and LYM, where only 180 H has an ultrasound signal. Again, a similar situation applies to parameters such as HGB and PDW, where only the highest ultrasound signal at 90 s (90 H) and 180 s (180 H) durations influences the values of the parameters. A review of all the blood parameters for which the null hypothesis is retained reveals that the parameter values at 90 H and 180 H slightly increase or decrease.

The boxplot diagrams in Figure 4 show the results of Kruskal–Wallis tests for different blood parameters for which the  $p$ -value is very low  $<0.001$  (null hypothesis is rejected) and the effect of ultrasound on these parameters is therefore most significant. In a set of 20 blood parameters, 5 of them responded quite severely to high-intensity ultrasound signals.

Analyzing the RBC values, we can observe that a strong ultrasound signal causes a sharp decrease in values, a medium intensity signal has almost no effect, and a weak one leads to a slight increase in values. A similar situation can be observed with the HTC parameter. From the results of MCH and MCHC parameters, we can see that, in contrast to RBC and HTC, a strong ultrasound signal leads to an increase in parameter values outside the normal range, including extreme values. In the case of the MID (%) parameter, there is also an increase in values when exposed to a strong ultrasound signal for both 90 and 180 s.

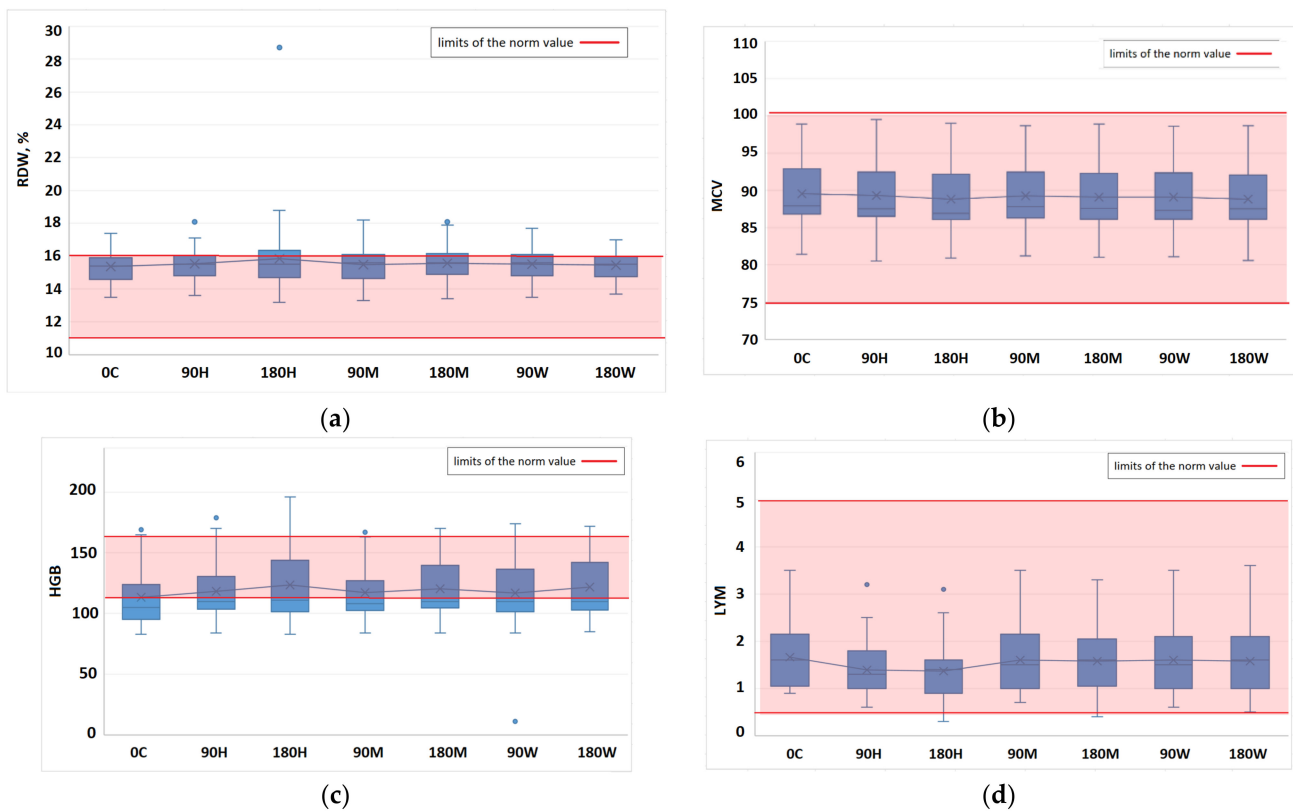


**Figure 3.** Independent-sample Kruskal–Wallis test results for four different blood parameters with a  $p$ -value of  $> 0.05$  (null hypothesis is retained). — the limits of the norm for a particular parameter, the norm area, which defines the normal range for the indicated blood parameter. (a) RDW parameter. (b) MCV parameter. (c) HGB parameter. (d) LYM parameter.

The research method of pairwise comparison of ultrasound signal values for the five most responsive blood parameters (RBC, HTC, MCH, MCHC, MID (%)) was applied and is shown in (Figure 5). With all other blood parameters, the same heptagon pattern was obtained, with all red linear connections.

The heptagon vertices depicted in Figure 5 correspond to the following ultrasonic exposure values: initial status (0 H); 1 (180 H); 2 (180 M); 3 (90 W); 4 (90 H); 5 (90 M); 6 (180 W). Different colors of the junctions between the peaks indicate different  $p$ -values between the pairs (the values of the corresponding blood parameter affected by the different ultrasound signals). If the line is blue, the  $p$ -value is  $< 0.05$ ; otherwise, the line is red. Nevertheless, our primary focus lies in the pairs featuring a zero-heptagon vertex, which refers to the initial values of the blood parameter. When considering a zero vertex, blue connections are frequently observed with vertices 4 (90 H) and 1 (180 H), which serve as indications of a high-intensity ultrasound signal lasting for 90 s and 180 s, respectively. Furthermore, there exists a more pronounced interdependence among vertices 1, 3, and 6.

More details are provided in Table 4, which shows the specific  $p$ -values adjusted with Bonferroni connection between the blood parameters' initial values and those exposed to different ultrasound signals. The table reveals a significant impact of the 90 H ultrasound signal on denoted blood parameter values. In contrast, medium ultrasound signals (90 M and 180 M) exhibit a considerably lower effect, and weak signals do not appear to have a significant influence on any of the five blood parameters. The graphs in Figure 6 show the results of the Kruskal–Wallis test for blood parameters with a significance level of  $> 0.05$ . It is evident that exposure to high-intensity 180 H and 90 H ultrasound signals can lead to both an increase and a decrease in parameter values.

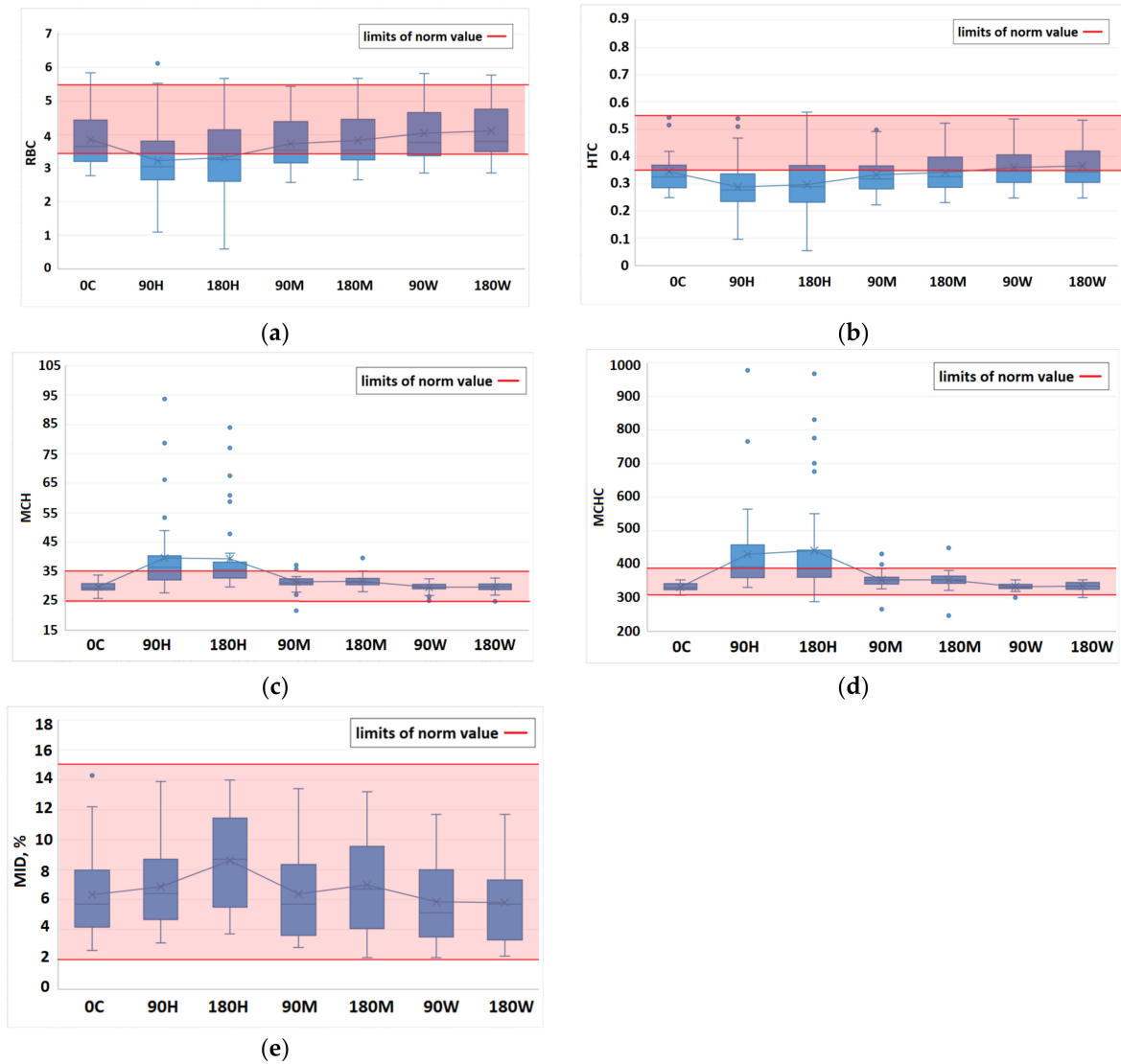


**Figure 4.** Independent-sample Kruskal–Wallis test results on different blood parameters with a very low  $p$ -value ( $< 0.001$ ). The red line — shows the limits of the norm for a particular parameter, the norm area, which defines the normal range for the denoted blood parameter. (a) RBC parameter. (b) HTC parameter. (c) MCH parameter. (d) MCHC parameter. (e) MID (%) parameter.

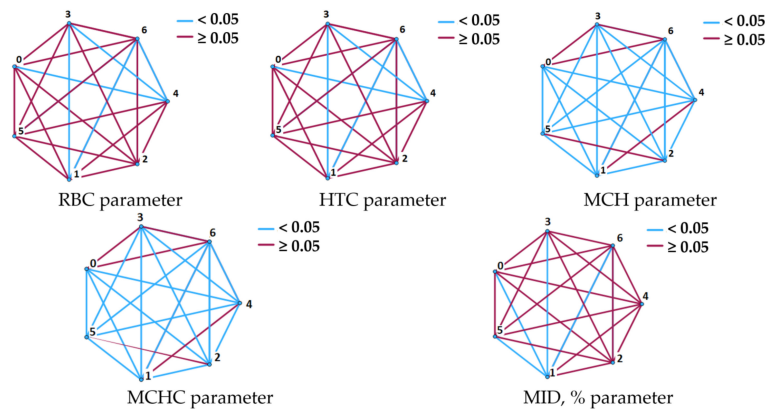


**Figure 5.** Pairwise comparison of each parameter (V1) where each node shows the sample average rank of V1. The vertices of the hexagon correspond to the following values of ultrasonic exposure: 0 (0 C); 1 (180 H); 2 (180 M); 3 (90 W); 4 (90 H); 5 (90 M); 6 (180 W).

**Table 4.** Dunn’s test results for the blood parameters most affected by ultrasound signals.

Blood Parameter	<i>p</i> -Values Adjusted by the Bonferroni Correction					
	0 C-180 W	0 C-90 M	0 C-180 H	0 C-90 H	0 C-90 W	0 C-180 M
RBC	1.000	1.000	0.469	0.037	1.000	1.000
HTC	1.000	1.000	0.324	0.047	1.000	1.000
MCH	1.000	0.008	0.000	0.000	1.000	0.03
MCHC	1.000	0.000	0.000	0.000	1.000	0.000
MID, %	1.000	1.000	0.028	1.000	1.000	1.000

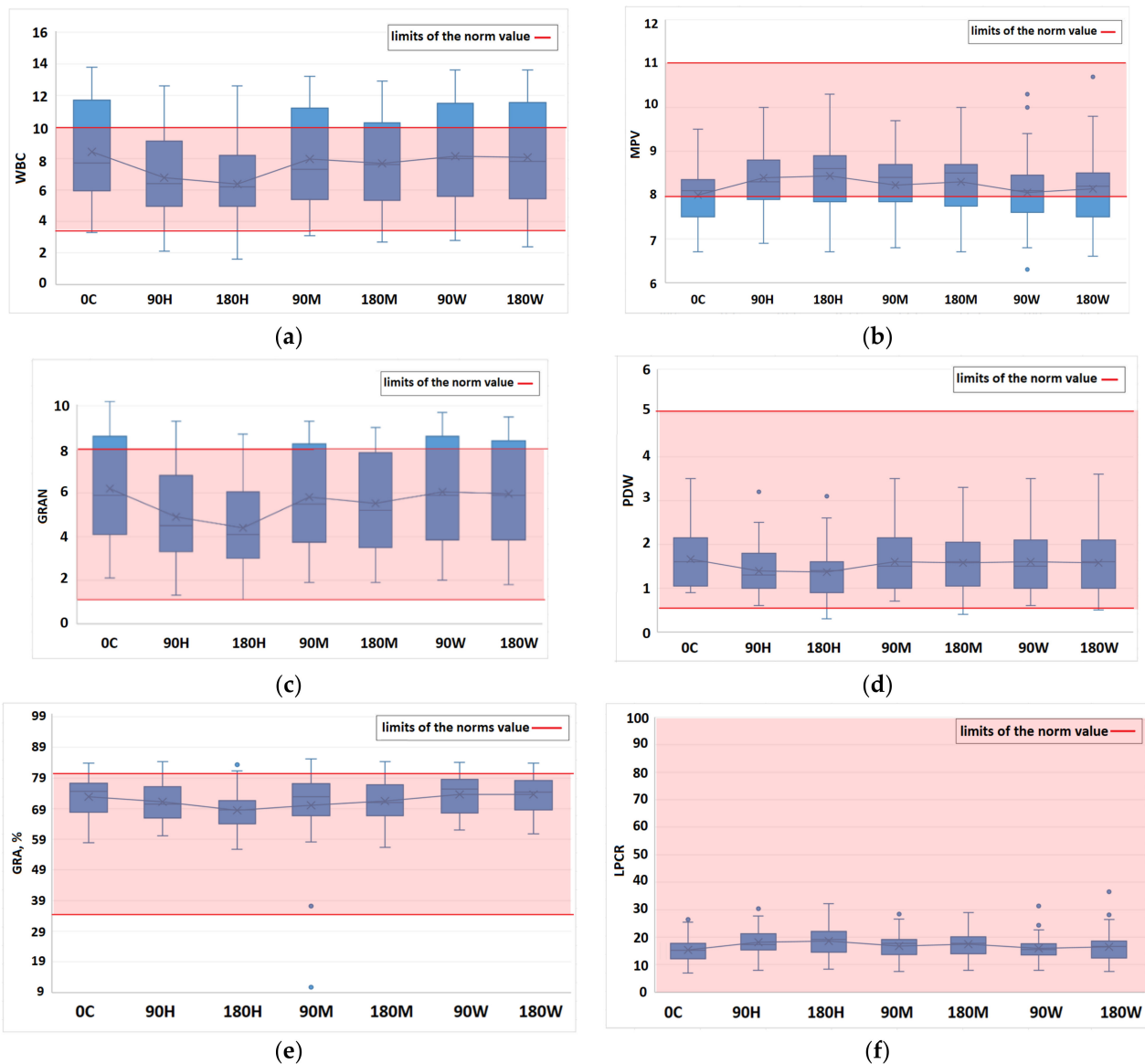


**Figure 6.** Independent-sample Kruskal-Wallis test results on different blood parameters with a  $p$ -value of  $< 0.05$ . The red line shows the limits of the norm for a particular parameter, the norm area. (a) WBC parameter with  $p$ -value = 0.010. (b) MPV parameter with  $p$ -value = 0.037. (c) GRAN parameter with  $p$ -value = 0.002. (d) PDW parameter with  $p$ -value = 0.044. (e) GRA (%) parameter with  $p$ -value = 0.006. (f) LPCR parameter with  $p$ -value = 0.015.

### 3.4. Platelet Number Prediction

Ongoing efforts are underway to predict platelet (PLT) values based on the influence of ultrasound signals, their duration, and intensity. Machine learning algorithms are well suited to PLT value predictions. Among the various algorithms used for regression problems, this study employed the five most popular ones. Based on the experimental results of 10 tests, the support vector regression (SVR) algorithm with a linear kernel was found to be the most accurate algorithm, as determined by the root mean square error (RMSE) metric.

Considering the results of all the machine learning algorithms, we can see that the highest error values are obtained with the three-layer ANN, with an average RMSE value of 72.47 for all six different ultrasound signals (Table 5). The largest prediction errors are observed for the high-impact signals, i.e., 90 H and 180 H, while the best prediction results are obtained for the PLT values after exposure to medium signals (90 M and 180 M). The same tendency can be seen with the remaining models. The LR, DT, and RF models have an average error of 55.50, 47.61, and 44.39, respectively, and SVR demonstrated the best prediction accuracy with an average RMSE of 32.06 (MAPE = 10.34%, Figure 7).

**Table 5.** PLT prediction results providing the average RMSE value obtained from 10 tests for five different ML algorithms: decision trees (DT), random forest (RF), artificial neural network (ANN), linear regression (LR), and support vector regression (SVR).

ML Algorithm	90 W	180 W	90 M	180 M	90 H	180 H
DT	44.156	36.61	41.61	35.8	67.34	60.16
RF	47.822	33.68	34.49	29.75	67.98	52.63
ANN	66.04	51.84	27.04	41.75	154.24	93.96
LR	48.99	42.83	43.54	38.77	76.05	82.83
SVR	23.45	27.73	22.90	27.12	35.41	55.80

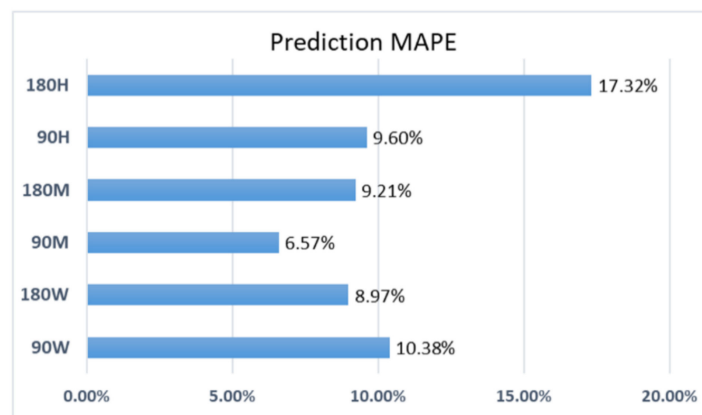


**Figure 7.** Prediction accuracy with an average MAPE.

Figure 8 shows the results of the SVR model’s prediction of the PLT value (in terms of the MAPE value) using different ultrasound signals. The best accuracy of 6.57% was obtained when predicting PLT values after exposure to the 90 M signal, while the worst accuracy of 17.32% was obtained when predicting the results after exposure to the 180 H signal. It can be assumed that the effect of a longer and stronger ultrasound signal is slightly more difficult to predict, as extreme values occur. This is also evident from the results in (a,b) of Figure 8, where the actual PLT values affected by the ultrasound signal are shown as blue dots and the predicted ones as red dots.

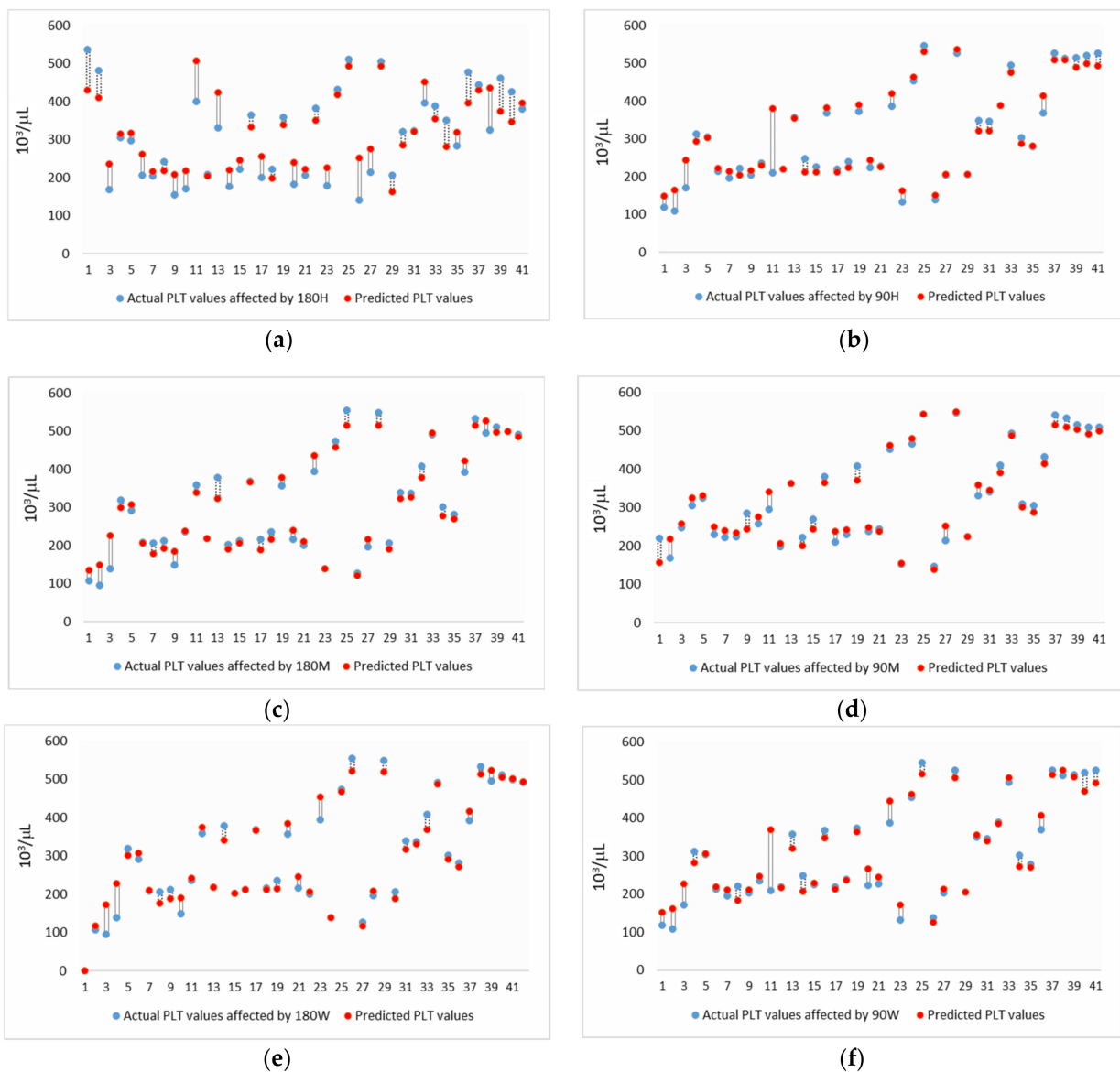


**Figure 8.** PLT prediction results for the test data using the SVR model with actual and predicted PLT values exposed to different ultrasound signals: (a) 180 H, (b) 90 H, (c) 180 M, (d) 90 M, (e) 180 W and (f) 90 W.

To assess the importance of attributes, we used the *F*-test statistical test [28], which is helpful for feature selection when there are numerous potential predictor factors, as we aim to identify a subset of variables that is most strongly associated with a response variable. The feature importance scores are computed as:

$$Fscore = -\log(p), \tag{4}$$

where *p* is the probability of *F*-test.

The top 5 importance scores of all blood parameters using the *F*-test algorithm for the prediction of the PLT value, including only the longest ultrasound signals of different strengths, i.e., 180 W, 180 M, and 180 H, are shown in Figure 9. These scores rank the attributes in order of importance, with a higher *F*-score indicating that the relevant predictor is more important. The results of the experiments showed that the baseline PLT value and the PCT are the blood factors that have the biggest impact on the predicted value of the PLT.

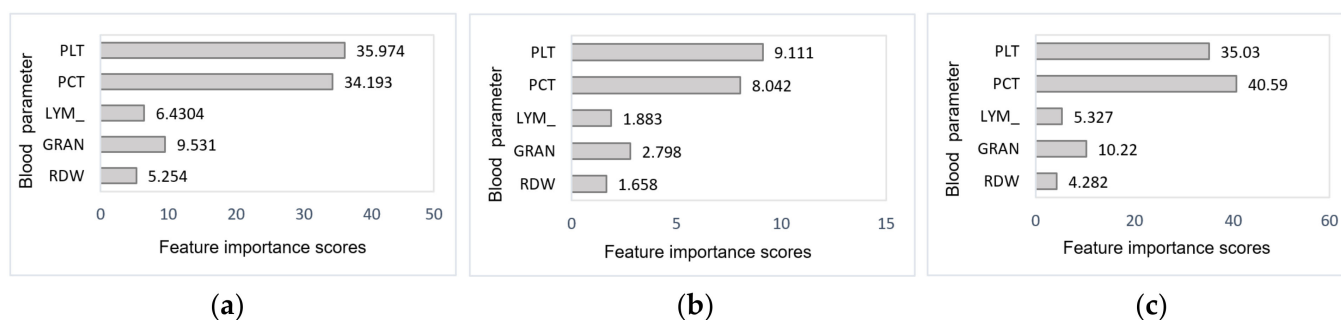


**Figure 9.** Feature importance scores ( $F$  scores) using the  $F$ -test algorithm for the PLT value prediction including 180 W, 180 M, and 180 H signals. (a) 180 W US signal. (b) 180 H US signal. (c) 180 M US signal.

#### 4. Discussion

The results of this study show that the observed changes in the parameters provided by the blood analyzer are not only related to the formation of blood clots, but also to the effects on red blood cells (RBCs). In addition to this fundamental finding, our research also aimed to propose faster statistical and artificial intelligence methods for processing blood parameters, avoiding the mistakes of inexperienced analysts. Ultrasound affects the blood by both radiation and flow forces. High-frequency ultrasound induces aggregation of blood particles by exciting standing acoustic waves in the liquid phase of the blood, where aggregated RBCs accumulate in the nodes. The aggregation of human RBCs is the major cause of a wide range of pathological conditions, from bacterial infections to cancer. In contrast to the standing waves caused by high-frequency ultrasound, low-frequency traveling acoustic waves cause the opposite phenomenon—the dissociation or mixing of RBC aggregates. Since blood is a shear-thinning fluid with complex reactions that strongly depend on the formation of aggregates by its components such as RBCs, the dissociation of RBC aggregates under the influence of low-frequency ultrasound begins as the shear rate increases above a critical value of  $\gamma = 5\text{--}10\text{ s}^{-1}$  [29]. Therefore, during blood analyzer tests, it was found that the number of single erythrocytes separated from aggregates by low-frequency ultrasound in the volume of a blood analyzer drop was higher than in the same volume of erythrocyte aggregates not affected by ultrasound.

Blood tests revealed that several parameters, such as mean corpuscular hemoglobin (MCH), the mean corpuscular hemoglobin concentration (MCHC), and platelet aggregation (PLT), show the greatest changes during exposure to low-frequency ultrasound and exceeded the permissible limits. The MCH and MCHC parameters indicate the amount of hemoglobin per cell and the amount of hemoglobin per unit volume, respectively. Hemoglobin is required to transport oxygen from the lungs to the cells of the body. Ultrasound has an impact on changes in these blood parameters related to RBC functions. During this study, venous blood was drawn from a vein near the elbow for laboratory purposes. Venous blood is low in oxygen. When ultrasound was used on dissociated erythrocytes in an open sample (surrounded by oxygen in a Vacuette K2E K2EDTA  $13 \times 75$  tube) and the shear rate exceeded a critical value, the color of the dissociated erythrocytes changed to a bright red color, as if they had been enriched by oxygen, as in the case of arterial blood. An important property of hemoglobin is that  $\text{O}_2$  binding is pH-dependent. It has been experimentally observed that  $\text{CO}_2$  is released more readily when the pH is acidic, i.e., when there are high concentrations of  $\text{CO}_2$ . This was the case for our blood samples before treatment with low-frequency ultrasound. This treatment has the potential to render hemoglobin more conducive to binding, with  $\text{CO}_2$  providing energy for the dispersion of gas bubbles within membranes or the fusion of multiple RBC membranes [30].

The key finding of this study was the observation of changes in gas exchange in the blood under the influence of different intensities of low-frequency ultrasound. This finding

holds potential implications for treating pulmonary hypertension using the low-frequency ultrasound transducer developed (patent pending) by the authors of this article [25].

#### *Suggestions for the Future*

The discovery that low-frequency ultrasound effects hemoglobin in RBCs (in vitro) to improve gas exchange has spurred us to start in vivo studies as soon as possible, and they are currently being prepared using the ultrasound transducer developed by the authors of this article [31] (patent pending). The clinical implications and therapeutic potential of ultrasound treatment in relation to these observed hematological changes need to be investigated. The mean, median, standard deviation, and interquartile range of blood parameters showed that ultrasound had an effect on granulocyte (GRAN) values as well as most other parameters. This parameter can be distinguished from the others because an increase in the granulocyte count indicates a bacterial infection [32]. However, statistically significant changes (decreases) in these values can be considered useful and may require further investigation, particularly regarding bacteria-related infectious blood tests. This finding suggests that ultrasound may have applications in the treatment of some bacterial diseases. Although ultrasound induces platelet aggregation, in vivo ultrasound may reduce the risk of thrombosis [33].

MCH and MCHC measure hemoglobin, which carries oxygen to the body's cells from the lungs, improving the absorption of iron [34], folate (B9), and cobalamin (B12) to stop bleeding or blood loss. Under the influence of ultrasound, an increase in PLT reduces bleeding or blood loss and destroys the *S. aureus* biofilm covering the surface of the prostheses, which increases antibiotic susceptibility [35]. Ultrasound is suitable for the treatment of endothelial dysfunction because it facilitates drug exposure to liver and kidney cells in order to identify clinically relevant biomarkers related to the function of these cells. Focused low-frequency ultrasound is a rapidly developing, non-invasive therapeutic technology that has the potential to improve the quality of life and reduce the cost of care for patients with heart valve calcification [36]. However, ultrasound can cause some biophysical effects, including thermal and non-thermal effects on cells, but these effects are significantly fewer with low-frequency ultrasound than with high-frequency ultrasound. Sonoporation, the most widely studied non-thermal biological effect of ultrasound, is considered to be a basis for new therapeutic applications. Ultrasound can increase the permeability of cell membranes due to the sonoporation effect, allowing molecules such as drugs, proteins, and DNA that cannot normally penetrate cell membranes to enter cells.

#### **5. Conclusions**

In this study, we conducted an evaluation of alterations in blood analysis data caused by the influence of ultrasound. Using an ANOVA and non-parametric Kruskal–Wallis statistical analyses, we confirmed significant changes in blood parameters due to exposure to 180 or 90 s of high- and medium-intensity ultrasound signals. The experimental results reveal that ultrasound signals have a statistically significant impact ( $p$ -value  $< 0.05$ ) on multiple blood parameters, with MCH emerging as the most sensitive among them, alongside RBC, HTC, MCHC, GRAN, and MID%. In contrast, RDW values, with a  $p$ -value of 0.990, exhibited minimal changes even under high-intensity signals (180 H and 90 H).

To predict PLT (platelet) counts, five distinct machine learning algorithms (decision trees (DT), random forest (RF), an artificial neural network (ANN), linear regression (LR), and support vector regression (SVR)) were employed in the study. The highest prediction errors were observed for high-intensity signals, i.e., 90 H and 180 H, while the most accurate predictions were observed for medium-intensity signals (90 M and 180 M). The three-layer ANN consistently produced the highest errors, with an average RMSE of 72.47 across all six different ultrasound signals, while the LR, DT, and RF models had average errors of 55.50, 47.61, and 44.39, respectively. The SVR model had the best prediction accuracy, with an average RMSE of 32.06 (MAPE = 10.34%). The lowest prediction error (MAPE), at 6.57%, was achieved when predicting PLT values exposed to the 90 M signal, while the lowest

accuracy, at 17.32%, was observed when predicting values exposed to the 180 H signal. It is essential to note that the prediction of PLT values has shown that PLT, PCT, and GRAN values are the blood factors with the most substantial impact on the predictive accuracy of PLT values.

Ultrasound application led to a dissociation of aggregated erythrocytes into single erythrocytes, while platelets, on the other hand, were more rapidly activated, but their activity was lower after induction with epinephrine. The dissociation of erythrocytes from the aggregated to the single state results in an increase in hemoglobin carrier gas, which allows therapeutic support for patients with pulmonary hypertension. The aggregation of platelets increases blood coagulation, which is useful for wound healing. As a result of this research, faster statistical and artificial intelligence methods have been proposed to speed up the analysis and interpretation of blood parameters, allowing us to avoid the mistakes of inexperienced analysts and to take timely actions to improve human health.

**Author Contributions:** Conceptualization, V.O.; methodology, V.O., V.L., E.S. and V.T.; formal analysis, V.O. and A.T.; investigation, V.O. and V.J.; resources, V.O. and E.S.; data curation, E.S.; statistical data analysis, A.P.-T. and M.V.; machine learning model realization, A.P.-T.; writing—original draft preparation, V.O., A.P.-T. and L.K.; writing—review and editing, V.O., A.P.-T. and L.K.; visualization, V.O. and A.P.-T.; supervision, V.O. All authors have read and agreed to the published version of the manuscript.

**Funding:** This research was funded by European Regional Development Fund (project No 01.2.2-LMT-K-718-05-0076) under grant agreement with the Research Council of Lithuania (LMTLT). Funded as European Union's measure in response to COVID-19 pandemic.

**Institutional Review Board Statement:** The study with human pulmonary arteries was conducted according to the principles defined in the Declaration of Helsinki [37]. Permission to perform this study was obtained from the local institutional review board of the Kaunas Regional Biomedical Research Ethics Committee (No. 2022-03-10 Nr. BE-2-39).

**Data Availability Statement:** The datasets used and analyzed during the current study are available from the corresponding authors on reasonable request.

**Conflicts of Interest:** The authors declare no conflict of interest.

## References

1. Nandi, S.; Mohanty, K.; Nellenbach, K.; Erb, M. Ultrasound enhanced synthetic platelet therapy for augmented wound repair. *ACS Biomater. Sci. Eng.* **2020**, *6*, 3026–3036. [[CrossRef](#)]
2. Voigt, J.; Wendelken, M.; Driver, V.; Alvarez, O.M. Low-frequency ultrasound (20–40 kHz) as an adjunctive therapy for chronic wound healing: A systematic review of the literature and meta-analysis of eight randomized controlled trials. *Int. J. Low. Extrem. Wounds* **2011**, *10*, 190–199. [[CrossRef](#)]
3. Otto, C.; Baumann, M.; Schreiner, T.; Bartsch, G.; Borberg, H.; Schmid-Schonbein, P. Standardized ultrasound as a new method to induce platelet aggregation: Evaluation, influence of lipoproteins and of glycoprotein IIb/IIIa antagonist tirofiban. *Eur. J. Ultrasound* **2001**, *14*, 157–166. [[CrossRef](#)]
4. Samal, A.B.; Adzerikho, I.D.; Mrochek, A.G.; Loiko, E.N. Platelet aggregation and change in intracellular Ca<sup>2+</sup> induced by low-frequency ultrasound in vitro. *Eur. J. Ultrasound* **2000**, *11*, 53–59. [[CrossRef](#)]
5. Guo, S.; Shen, S.; Wang, J.; Wang, H.; Li, M.; Hou, F.; Liao, Y.; Bin, J. Detection of high-risk atherosclerotic plaques with ultrasound molecular imaging of glycoprotein IIb/IIIa receptor on activated platelets. *Theranostics* **2015**, *5*, 418–430. [[CrossRef](#)]
6. Tian, J.; Weng, Y.; Sun, R.; Zhu, Y.; Zhang, J.; Liu, H. Contrast-enhanced ultrasound molecular imaging of activated platelets in the progression of atherosclerosis using microbubbles bearing the von willebrand factor A1 domain. *Exp. Ther. Med.* **2021**, *2*, 721. [[CrossRef](#)]
7. Signori, L.U.; Teixeira, A.O.; da Silva, A.M.V.; da Costa, S.T. Effects of therapeutic ultrasound on hematological dynamics and fibrinogen during the inflammatory phase after muscle injury in rats. *Acta Sci. Health Sci.* **2014**, *36*, 25–31. [[CrossRef](#)]
8. Cherniavsky, E.A.; Strakha, I.S.; Adzerikho, I.E.; Shkumatov, V.M. Effects of low-frequency ultrasound on some properties of fibrinogen and its plasminolysis. *BMC Biochem.* **2011**, *12*, 60. [[CrossRef](#)]
9. Ivone, M.; Pappalettere, C.; Watanabe, A.; Tachibana, K. Study of cellular response induced by low intensity ultrasound frequency sweep pattern on myelomonocytic lymphoma U937 cells. *J. Ultrasound* **2016**, *19*, 167–174. [[CrossRef](#)]

10. Qin, H.; Du, L.; Luo, Z.; He, Z.; Wang, Q.; Chen, S.; Zhu, Y.-L. The therapeutic effects of low-intensity pulsed ultrasound in musculoskeletal soft tissue injuries: Focusing on the molecular mechanism. *Front. Bioeng. Biotechnol.* **2022**, *10*, 1080430. [[CrossRef](#)]
11. Garavand, A.; Behmanesh, A.; Aslani, N.; Sadeghsalehi, H.; Ghaderzadeh, M.; El Kafhali, S. Towards diagnostic aided systems in coronary artery disease detection: A comprehensive multiview survey of the state of the art. *Int. J. Intell. Syst.* **2023**, *2023*, 6442756. [[CrossRef](#)]
12. Ghadezadeh, M.; Mehrad, A.; Azamossadat, H.; Farkhondeh, A.; Davood, B.; Hassan, A. A fast and efficient CNN model for B-ALL diagnosis and its subtypes classification using peripheral blood smear images. *Int. J. Intell. Syst.* **2021**, *37*, 5113–5133. [[CrossRef](#)]
13. Varghese, N.E. Machine learning techniques for the classification of blood cells and prediction of diseases. *Int. J. Comput. Sci. Eng.* **2020**, *9*, 66–75.
14. Amato, F.; Lopez, A.; Pena-Mendez, E.M.; Vanhara, P.; Hampel, A.; Havel, J. Artificial neural networks in medical diagnosis. *J. Appl. Biomed.* **2013**, *11*, 47–58. [[CrossRef](#)]
15. Alsheref, F.K.; Gomaa, W.H. Blood diseases detection using classical machine learning algorithms. *Int. J. Adv. Comput. Sci. Appl.* **2019**, *10*, 77–81. [[CrossRef](#)]
16. Neeb, H.; Grieger, S.; Luxem, K.; Strasser, E.F.; Kraus, M.-J. Active or not—Machine-learning based prediction of platelet activation. In Proceedings of the World Congress on Engineering and Computer Science 2014, San Francisco, CA, USA, 22–24 October 2014; Volume I.
17. Jiang, Y.; Lei, C.; Yasumoto, A.; Kobayashi, H.; Aisaka, Y.; Ito, T.; Guo, B.; Nitta, N.; Kutsuna, N.; Ozeki, Y.; et al. Label-free detection of aggregated platelets in blood by machine-learning-aided optofluidic time-stretch microscopy. *Lab Chip* **2017**, *17*, 2426–2434. [[CrossRef](#)]
18. Matsuo, H.; Kamada, M.; Imamura, A.; Shimizu, M.; Inagaki, M.; Tsuji, Y.; Hashimoto, M.; Tanaka, M.; Ito, H.; Fujii, Y. Machine learning-based prediction of relapse in rheumatoid arthritis patients using data on ultrasound examination and blood test. *Sci. Rep.* **2022**, *12*, 7224. [[CrossRef](#)]
19. Sampathila, N.; Chadaga, K.; Goswami, N.; Chadaga, R.P.; Pandya, M.; Prabhu, S.; Bairy, M.G.; Katta, S.S.; Bhat, D.; Upadya, S.P. Customized deep learning classifier for detection of acute lymphoblastic leukemia using blood smear images. *Healthcare* **2022**, *10*, 1812. [[CrossRef](#)]
20. Hu, Y.; Luo, Y.; Tang, G.; Huang, Y.; Kang, J.; Wang, D. Artificial intelligence and its applications in digital hematopathology. *Blood Sci.* **2022**, *4*, 136–142. [[CrossRef](#)]
21. Swelab Alfa Plus User's Manual. Available online: <https://boule.com/document-folder/?id=230> (accessed on 12 June 2023).
22. Riffenburgh, R.H. *Statistics in Medicine*, 3rd ed.; Academic Press: Cambridge, MA, USA, 2012.
23. Sherwani, R.A.K.; Shakeel, H.; Awan, W.B.; Faheem, M.; Aslam, M. Analysis of COVID-19 data using neutrosophic Kruskal Wallis H test. *BMC Med. Res. Methodol.* **2021**, *21*, 215. [[CrossRef](#)]
24. Bayram, M.; Bayraktar, G.; Akyol, H.; Can, B. Comparing some blood parameters of ski racers and long-distance athletes. *Turk. J. Sport Exerc.* **2017**, *19*, 331–336. [[CrossRef](#)]
25. Knapp, H. *Intermediate Statistics Using SPSS*, 1st ed.; SAGE Publications: Thousand Oaks, CA, USA, 2017; p. 480.
26. Botchkarev, A. Performance metrics (error measures) in machine learning regression, forecasting and prognostics: Properties and typology. *Interdiscip. J. Inf. Knowl. Manag.* **2019**, *14*, 45–79.
27. Palma-Barqueros, V.; Revilla, N.; Sánchez, A.; Zamora Cánovas, A.; Rodríguez-Alén, A.; Marín-Quílez, A.; González-Porras, J.R.; Vicente, V.; Lozano, M.L.; Bastida, J.M.; et al. Inherited Platelet Disorders: An Updated Overview. *Int. J. Mol. Sci.* **2021**, *22*, 4521. [[CrossRef](#)] [[PubMed](#)]
28. Mahbobi, M.; Tiemann, T.K. *Introductory Business Statistics with Interactive Spreadsheets*, 1st Canadian ed.; BCcampus: Victoria, BC, Canada, 2015; p. 102.
29. Yeom, E.; Nam, K.H.; Paeng, S.J. Effects of red blood cell aggregates dissociation on the estimation of ultrasound speckle image velocimetry. *Ultrasonics* **2014**, *54*, 1480–1487. [[CrossRef](#)] [[PubMed](#)]
30. Vidallon, M.L.P.; Tabor, R.F.; Bishop, A.I.; Teo, B.M. Ultrasound-assisted fabrication of acoustically active, erythrocyte membrane “bubbles”. *Ultrason. Sonochem.* **2021**, *72*, 105429. [[CrossRef](#)]
31. Ostasevicius, V.; Jurenas, V.; Mikuckyte, S.; Vezys, J.; Stankevicius, E.; Bubulis, A.; Venslauskas, M.; Kizauskiene, L. Development of a low-frequency piezoelectric ultrasonic transducer for biological tissue sonication. *Sensors* **2023**, *23*, 3608. [[CrossRef](#)]
32. Van der Geest, A.P.J.; Mohseni, M.; Brower, R.; Van der Hoven, B.; Steyerberg, L.W.; Groeneveld, A.B.J. Immature granulocytes predict microbial infection and its adverse sequelae in the intensive care unit. *J. Crit. Care* **2014**, *29*, 523–527. [[CrossRef](#)]
33. Wang, Z.; Pan, Y.; Huang, H.; Zhang, Y.; Li, Y.; Zou, C.; Huang, G.; Chen, Y.; Li, Y.; Li, J.; et al. Enhanced thrombolysis by endovascular low-frequency ultrasound with bifunctional microbubbles in venous thrombosis: In vitro and in vivo study. *Front. Bioeng. Biotechnol.* **2022**, *10*, 965769. [[CrossRef](#)]
34. Wallace, D.F. The regulation of iron absorption and homeostasis. *Clin. Biochem. Rev.* **2016**, *37*, 51–62.
35. Erriu, M.; Blus, C.; Szmukler-Moncler, S.; Buogo, S.; Levi, R.; Barbato, G.; Madonnaripa, D.; Denotti, G.; Piras, V.; Orrù, G. Microbial biofilm modulation by ultrasound: Current concepts and controversies. *Ultrason. Sonochem.* **2013**, *21*, 15–22. [[CrossRef](#)]

36. Messas, E.; Ijsselmuiden, A.; Goudot, G.; Vlieger, S.; Den Heijer, P.; Puymirat, E.; Spaulding, C.; Zarka, S.; Hagege, A.A.; Marijon, E.; et al. Safety, feasibility and performance of valvsoft non-invasive ultrasound therapy in patients with severe symptomatic calcific aortic valve stenosis. First-in-Man. *Eur. Heart J.* **2020**, *41*, ehaa946.1932. [[CrossRef](#)]
37. Carlson, R.V.; Boyd, K.M.; Webb, D.J. The revision of the declaration of Helsinki: Past, present and future. *Br. J. Clin. Pharmacol.* **2004**, *57*, 695–713. [[CrossRef](#)] [[PubMed](#)]

**Disclaimer/Publisher's Note:** The statements, opinions and data contained in all publications are solely those of the individual author(s) and contributor(s) and not of MDPI and/or the editor(s). MDPI and/or the editor(s) disclaim responsibility for any injury to people or property resulting from any ideas, methods, instructions or products referred to in the content.